This is an *Accepted Manuscript*, which has been through the Royal Society of Chemistry peer review process and has been accepted for publication.

Accepted Manuscripts are published online shortly after acceptance, before technical editing, formatting and proof reading. Using this free service, authors can make their results available to the community, in citable form, before we publish the edited article. We will replace this *Accepted Manuscript* with the edited and formatted *Advance Article* as soon as it is available.

You can find more information about *Accepted Manuscripts* in the **Information for Authors**.

Nanoscale

ARTICLE

Flexible, Transparent and Exceptionally High Power Output Nanogenerators Based on Ultrathin ZnO Nanoflakes

Huynh Van Ngoc and Dae Joon Kang*

Novel nanogenerator structures composed of ZnO nanoflakes less than 10-nm thick were fabricated using a novel method involving a facile synthetic route and rational design. The fabricated nanogenerators exhibited a short-circuit current density of 67 μA cm^{-2}, a peak to peak open-circuit voltage of 110 V, and an overall output power density exceeding 1.2 mW cm^{-2}, and to the best of our knowledge, these are the best values that have been reported so far in the literature on ZnO-based nanogenerators. We demonstrated that our nanogenerator design could instantaneously power 20 commercial green light-emitting diodes without any additional energy storage processes. Both the facile synthetic route for the ZnO nanoflakes and the straightforward device fabrication process present great scaling potential in order to power mobile and personal electronics that can be used in smart wearable systems, transparent and flexible devices, implantable telemetric energy receivers, electronic emergency equipment, and other self-powered nano/micro devices.

Introduction

Mechanical energy can be artificially generated from vibration, sound waves, automobile movement, and human motion, yet this energy is usually wasted. Recently, the idea of scavenging ambient mechanical energy has become an attractive alternative for wireless sensing, implanted medical devices, and portable smart electronics since these are experiencing a rapid increase in use. Furthermore, this method has become more realistic as the technology of nanoelectronics advances. These devices have extremely low power consumption, so energy harvested from the environment may be sufficient for these portable devices to operate.

There is a growing interest in NGs that harvest mechanical energy through piezoelectric or triboelectric processes,[1] and in addition to piezoelectricity, triboelectric means have recently gained a considerable attention because these processes greatly improve the power output.[2–4] However, triboelectricity requires the electrodes to be mechanically separated, creating an air gap that maintains and isolates the electrostatic charges to form dipole moment. This requires a device with a relatively large size, and the device must additionally contain a limited maximum number of layers in its vertical stack to obtain high output-power NGs. Therefore, piezoelectricity is considered to be the best operating

mechanism to produce viable self-powered devices because this mechanism relies on small components (including a sensor or an actuator), and it is suitable for use in high power output applications.

One-dimensional ZnO nanostructures have a non-centrosymmetric structure and fascinating properties and as a result have been extensively studied as active materials for use in NGs.[5] The unique coupling of the piezoelectric and the semiconducting properties of the ZnO-based NGs produces a much larger output current than that obtained with insulating piezoelectric materials, such as lead zirconate titanate (PZT) and barium titanate (BTO). However, free charge carriers that are available in semiconducting ZnO create a screening effect for the piezoelectric potential, resulting in a poor output power. Various strategies, such as a Schottky barrier contact,[6–9] a thin insulating layer,[10–15] separation of charge accumulation,[11,16] a p-n junction,[17,18] and hybridization of two piezoelectric materials,[19] have been proposed to avoid the screening effect and to improve the output power of the NGs. However, these approaches have experienced limited success, and many of these experiments are involved in structures based on ZnO nanowire (NW).[20,21] Very recently, ZnO nanoflakes (NFs) have attracted great scientific interest as the building blocks for high-output-power NGs since their unique structures produce a high output current.[22] In particular, the dominant surface piezoelectricity that is inherent to NF structures may produce a significant piezoelectric effect when the thickness of the NFs is reduced below 30 nm.[23,24]

In this study, we report on a novel and simple synthetic route to obtain ultrathin ZnO NFs that can be grown on arbitrary substrates by using an aqueous precipitation method at room temperature. Microscopic observations revealed that the NFs had plate-like morphologies with a thickness under 10 nm, which is expected to play a vital role in power generation and device performance. Thus,

Department of Physics, Sungkyunkwan University, Suwon 440-746, Republic of Korea. E-mail: djkang@skku.edu; Fax: +82-31-290-5947; Tel: +82-31-290-5906

this novel structure was exploited to obtain high-power-output NGs, and ZnO nanowire-based NGs (NWNGs) were also fabricated for comparison. The experimental results were further verified by using different vibration sources, including the periodic pounding of a heavy object as well as a sound wave. Different interface mechanisms, such as thin insulating layers, a p-n junction, and the hybridization of two piezoelectric materials were experimentally compared to maximize the piezoelectric output power and are discussed here in detail. We obtained the best results by hybridizing two piezoelectric materials comprising ZnO NFs coated with organic piezoelectric poly(vinylidene fluoride-trifluoroethylene) [P(VDF-TrFE)]. The hybridizing nanogenerators exhibited a short-circuit current density of 80 µA cm^{-2}, a peak to peak open-circuit voltage of 127 V, and an overall output power density exceeding 1.6 mW cm^{-2}. The fabricated device had an area of 4 × 4 cm^2, and the output power of our NG was used directly to instantly turn on 60 commercial light-emitting diodes (LEDs) without the use of any other energy storage systems.

Experimental

### Synthesis of ZnO nanoflakes

Zinc acetate dihydrate [Zn(CH$_3$COO)$_2$·2H$_2$O] and sodium hydroxide (NaOH) reagents were purchased from Sigma-Aldrich, Korea and were used without further purification. The seed layer was formed by dipping the substrate in a 5-mM zinc acetate dihydrate solution (i.e., zinc acetate dihydrate dissolved in high-grade ethanol) and then baking the layer on a hot plate at 150 °C for 5 min to uniformly grow ZnO NFs on a large-area substrate. This step was repeated three times to ensure uniform coating. ZnO NFs were successfully synthesized from the seed layer using a room-temperature aqueous precipitation method. In a typical process, 1 mL of 1 M zinc acetate aqueous solution was added to 1 mL of 8 M NaOH aqueous solution, and then stirred for 10 min. The solution was diluted in a 200 mL aqueous solution by suspending the substrates upside down in a glass bottle filled with the solution and was then stirred vigorously for 2 min. The aforementioned solution was then diluted again in an 800 mL aqueous solution for 1 h. The substrate was rinsed with deionized water and was then heated on a hot plate at 150 °C for 2 h. The ZnO NFs were grown on three different substrates: (1) a transparent conductive polyethylene terephthalate (PET) plastic substrate coated with indium tin oxide (ITO), (2) a glass substrate coated with fluorine-doped tin oxide (FTO), and (3) a woven textile substrate of Au-coated synthetic polyester fibers. The electrical characteristics of the NG devices were measured using an oscilloscope (LeCroy WavePro 715Zi) and a low-noise current preamplifier (Stanford Research Systems SR570).

Results and discussion

Structural characterization of ZnO nanoflakes

The morphology of the ZnO NFs was examined by using field-emission scanning electron microscopy (FE-SEM) (JEOL JSM-7401F). The SEM images of the ZnO NFs show high-density ZnO NFs with uniform growth and full coverage of the textile (Fig. 1a) and ITO/PET (Fig. 1b) substrates of approximately 50 cm^2 each. High-

resolution SEM images of the individual ZnO NFs are shown in the insets, and these indicate that the ZnO NF comprise a plate that has less than 10 nm thickness, 500 nm height, and 1 µm length (Fig. S1 in ESI†). Meanwhile, the same ZnO NF structure was also grown on an FTO/glass substrate (Fig. S1c,d in ESI†).
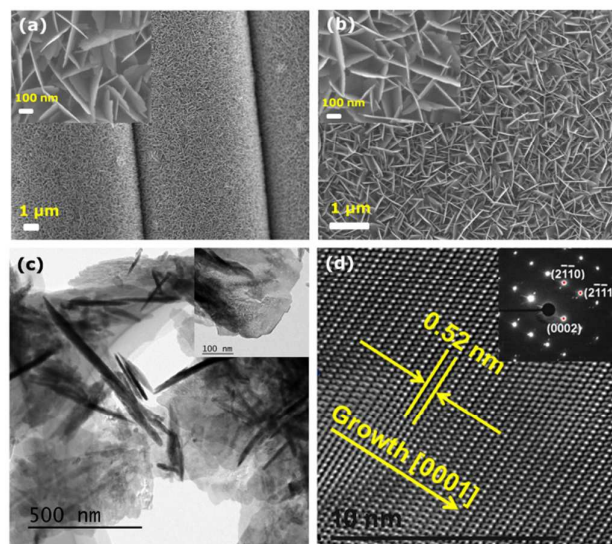

Fig. 1 FE-SEM images of ZnO NFs on (a) textile and (b) ITO/PET substrates. (c) TEM image and (d) HRTEM image of ZnO NFs (inset depicting SAED pattern).

The crystalline nature of the ZnO NFs was further examined via high-resolution transmission electron microscopy (HRTEM, FE-TEM JEM2100F). Fig. 1c shows a typical TEM image of a single hexagonal ZnO nanoplate. Due to the ultrathin plate thickness (less than 10 nm), the plate was highly transparent to an electron beam. The inset in Fig. 1d shows a selective-area electron diffraction (SAED) pattern that is recorded by aligning the electron beam that is perpendicular to the side-face of the NF. The diffraction pattern indicates growth in the [0001] direction, and a high-quality single-crystalline phase is dominated by (0002) facets. The corresponding HRTEM image (Fig. 1d) of the selected area of the ZnO NF (marked by a square in Fig. 1c) further confirmed the single-crystalline hexagonal structure of the NFs. Clear lattice fringes with a spacing of 0.52 nm correspond to the (0001) crystal planes. Therefore, the TEM results confirmed that the preferred growth direction of the ZnO NFs was along the c-axis of the hexagonal cell, and this orientation shows the best piezoelectric coefficient response for the ZnO NF-based power generator. The X-ray diffraction (XRD) (D8 FOCUS 2200 V, Bruker AXS) spectrum taken from the NFs further confirmed their single-crystalline ZnO structures, as shown in the ESI Fig. S2.†

Device structure and operating mechanism of NF-based NGs (NFNGs)

The NG device structure and the corresponding optical image are shown in Fig. 2a and b. The fabrication process for the NG was conducted as follows. First, the ZnO NFs were grown on a commercially available conducting FTO/glass substrate. The FTO

Nanoscale Accepted Manuscript

layer was then used as a bottom electrode, and polydimethylsiloxane (PDMS) sols were prepared using a one-pot sol-gel process in which tetraethyl orthosilicate was used as an inorganic precursor and hydroxyl-terminated PDMS was used as an organic modifier with a weight ratio of 10:1. Dip-coating was then used to prepare a 2-μm-thick PDMS layer on the ZnO NFs with the sols. Finally, an ITO/PET layer was added on top of the PDMS. The ITO layer was employed as the top electrode for subsequent electrical measurements.
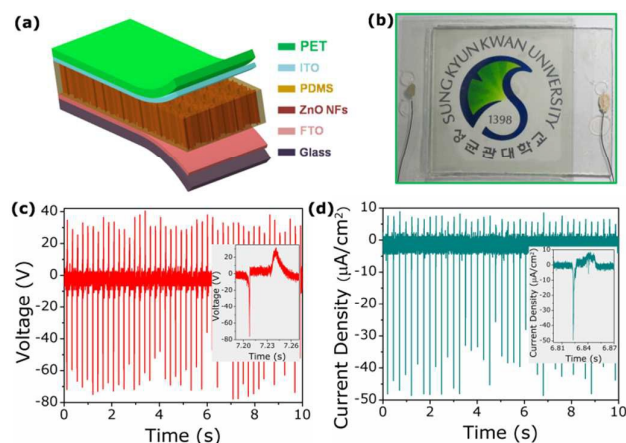
Fig. 2 ZnO NF-based NGs. (a) Device structure and (b) photographic image, (c) open-circuit voltage and (d) short-circuit current density of PDMS-coated ZnO NF-based NGs.

This facile and low-temperature growth process for ZnO NFs enabled us to grow ZnO NFs on both sides of the substrates, and the NGs could therefore be fabricated in multiple layers with a low thickness, thus presenting a great advantage in terms of a capability for both three-dimensional device scale-up and cost reduction. Fig. 2b shows an optical image of the NG. The under-500-nm-thick layer of the ZnO NFs with high-transparency PDMS and electrodes made our devices become almost transparent to visible light. Therefore, these devices are suitable for applications that require transparent NGs.

We prepared 1×1 cm^2 NG devices to systematically investigate the electrical properties of the NFNGs. The operating mechanism for the NFNGs was proposed by Falconi *et al.*[22] and is based on the transient flow of the inductive charges that are driven by the piezoelectric potential.[12,14,25] A piezoelectric potential is generated along the NFs when the device is compressed by a heavy object, and consequently, an electrostatic force is exerted on the top and bottom electrodes to drive mobile free electrons through an external load. To balance this piezoelectric potential, these electrons then accumulate at the interface between the NFs and the electrodes, and the piezoelectric potential is removed when the NFs decompress after removing the heavy object with the accumulated electrons flowing back through the external load. Therefore, both positive and negative currents and voltages can be observed.

Under the periodic impact of a heavy object (at a frequency of 4 Hz) and a constant force (at a maximum of 30 N), the NFNG devices exhibited a maximum peak to peak open-circuit voltage of 110 V

over a single pressing and releasing load cycle (which is 2.9 times higher than the best value reported to date in the literature, as shown in Fig. 2c)[11] and a short-circuit current density of 57 μA cm^{-2} (4.7 times higher than the best value obtained from the integrated ZnO NWNG devices, as shown in Fig. 2d).[11] The effective output power density (P) of the NGs was calculated as P = U^2/RA ,[26] where U is the output voltage, R is the load resistance, and A is effective size of the NGs. Our oscilloscope (LeCroy WavePro 715Zi) has input resistance of 10 MΩ, therefore we can estimate the maximum output power density of ~ 1.2 mW cm^{-2} in the case of PDMS-coated ZnO NFNG. The insets of Fig. 2c and d show the asymmetric shapes of the output voltage and the current that may result from the asymmetric nature of pressing and removing the heavy object. Specifically, the compression and decompression of the NFs was not symmetrical. Higher and narrower peaks were also observed when compression occurred more quickly than decompression, and the magnitude of both the output voltage and the current depended strongly on the compression pressure and frequency. We believe that the high output voltage is a result of the high surface area of the device and that the surface piezoelectricity originated from the ultrathin NFs.

Nanomaterials are known to exhibit size-dependent mechanical and physical properties as a result of their large surface-area-to-volume ratios. Experimental studies and atomistic simulations have demonstrated that the piezoelectric coefficients of some piezoelectric materials may dramatically increase when the sample is reduced to the nanometer scale.[27–30] A larger surface-area-to-volume ratio also contributes to the increase in the piezoelectric coefficient. We performed Brunauer-Emmett-Teller (BET) nitrogen adsorption isotherm measurements for the ZnO NF and ZnO NW samples in order to estimate their surface areas. The BET results revealed the ZnO NFs had a specific surface area of about 25 m^2 g^{-1}, which are twelve orders of magnitude larger than that of the ZnO NWs (Fig. S3 in ESI†). We believe that the higher specific surface area of the ZnO NFs is significant in improving their piezoelectric response.
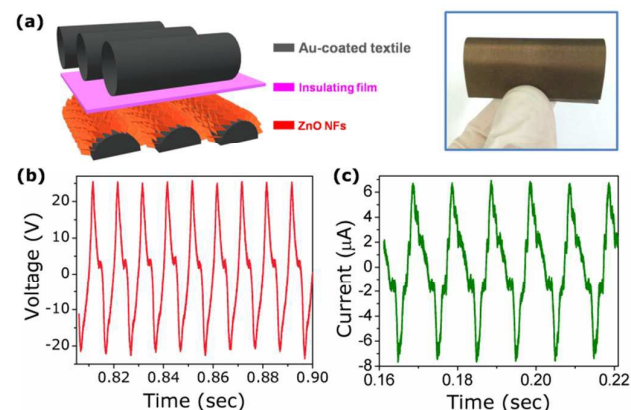
Fig. 3 Sound-driven textile NFNG and device application. (a) Device structure and photographic image, (b) open-circuit voltage, and (c) short-circuit current density of textile NFNG.

Yan, Zhang *et al*. used the Kirchhoff plate theory based on a surface piezoelectricity model and the generalized Young-Laplace

ARTICLE   Journal Name

equations to study the effect of the surface piezoelectricity on the NFs.[23,24] The surface piezoelectricity effects were more prominent for thinner NFs with larger aspect ratios.[23] As noted by Tagantsev *et al.*,[31] the effect of the surface piezoelectricity may become more significant when nanoscale piezoelectric materials are used. Yan *et al.* claimed that, relative to the residual surface stress and surface elasticity, the surface piezoelectricity can be significantly improved for NFs thinner than 30 nm.[23] The influence of the surface effects diminished as the plate thickness increases, and with NFs thinner than 10 nm, the surface piezoelectricity is expected to be greatly enhanced. Kim *et al.* experimentally reported on similarly-structured NFs.[32] The NG based on these NFs had a maximum output short-circuit current density of 16 µA cm^{-2}, which exceeded the value obtained using NW-based NG devices,[11] but it remained far below our results. This could be due to the lack of surface piezoelectricity effects when the thickness of the NFs reaches 80 nm.[32] Therefore, strong dominating surface piezoelectricity effects may account for an exceptionally high output voltage and current produced by our NFNGs, as compared to other reports on ZnO NW-based NGs with diameters above 50 nm,[10–12,19,33] as well as for NFs.[32,34] We notably obtained both a high output voltage and an unprecedentedly high output current that is 4.7 times larger than that obtained by other NWNGs.[11] Falconi *et al.* suggested that this NF structure was equivalent to a large number of NWs that are connected in parallel, which subsequently increases the maximum output current, and this provides guidance for both the design of highly efficient energy harvesting devices and the development of novel fabrication procedures.[22] We also suspect that this may contribute to the high output current that was obtained using our NFNGs.
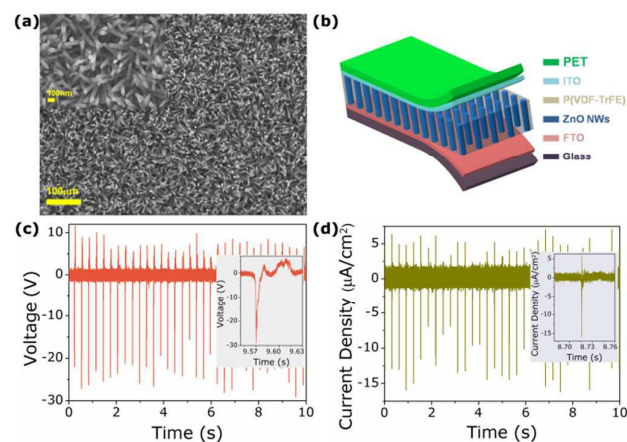
Fig. 4 ZnO NW-based NGs. (a) FE-SEM images of ZnO NWs on FTO/glass substrate, (b) device structure, (c) open-circuit voltage, and (d) short-circuit current density of P(VDF-TrFE)-coated ZnO NW-based NGs.

Different coating layers, including poly(methyl methacrylate) (PMMA), poly(3-hexylthiophene-2,5-diyl) (P$_3$HT) and ferroelectric P(VDF-TrFE), were applied to the ZnO NFs to determine the effect of the coating layer on the maximum piezoelectric output power. To date, four mechanisms have been proposed to account for the improved piezoelectric behavior of the NGs based on ZnO with

coating layers: (1) a Schottky barrier between metal-semiconductor contacts,[1–4] (2) a thin insulating layer replacing the Schottky contact to prevent current leakage through an internal structure,[10,11] (3) a thin insulating layer combined with the hybridization of two different piezoelectric materials,[19] and (4) a p-type polymer layer on a piezoelectric semiconducting layer.[17] We thus examine the validity of these mechanisms for our devices in the following subsections.
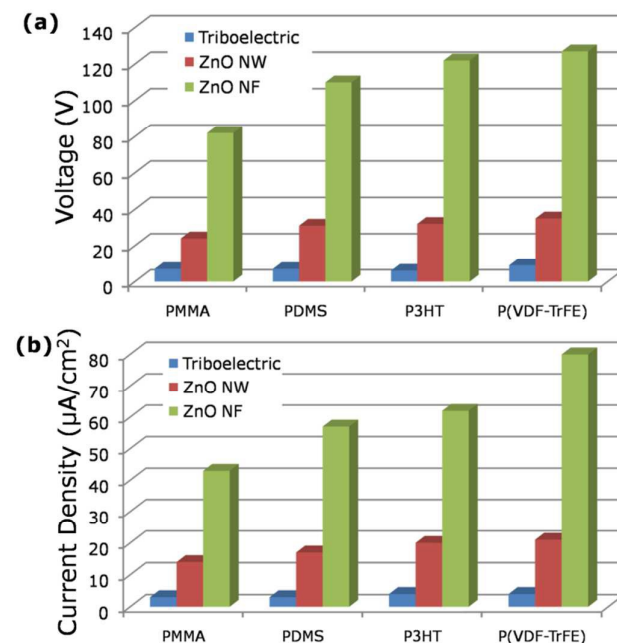
Fig. 5 NG performance based on the different effects of the piezoelectricity of ZnO NFs, the piezoelectricity of ZnO NWs, and triboelectricity. (a) Open-circuit voltage, and (b) short-circuit current density of PMMA, PDMS, P$_3$HT, and P(VDF-TrFE) coatings on NF/NW-based NGs.

Schottky contact

Optimizing both the conductivity and the carrier density of the ZnO is important in various piezoelectric applications. The electrostatic potential that is produced by the piezoelectric potential generated along the NFs from their mechanical deformation is established on the top and bottom electrodes of the NG device, and if the ZnO form an Ohmic contact with the electrodes, a conducting load will be produced due to the potential difference between the two electrodes, which screens the piezoelectric effect. To avoid this shorting issue, a Schottky barrier that depends on the size of the work function between the piezoelectric semiconductor and the metal electrode is formed. The Schottky barrier must be sufficiently high to prevent the charges from leaking.[35] For the ZnO, the Schottky barrier forms between the ZnO and the gold electrode because gold has a higher work function than the ZnO.[6–9] However, due to oxygen defects and Zn insertions, ZnO is well-known to be a natural n-type semiconductor. The conductivity of ZnO is quite high when compared to other piezoelectric metal oxides, and this reduces the thickness of the depletion layer such that the electrons

can easily tunnel through the Schottky barrier and then screen the effect of the piezoelectric potential. This screening issue can be resolved by adding a thin insulating layer between the piezoelectric semiconductor and the metal electrode, as is discussed below.

Thin insulating layer

The addition of a thin insulting layer between the piezoelectric semiconductor and the metal electrode can be quite effective in addressing the aforementioned screening issue. The layer provides a potential barrier with infinite height and width, preventing the electrons in the electrodes from tunneling through the Schottky barrier that is established at the semiconductor and metal interface.[10–15] In particular, a thin PMMA layer between the NFs and the metal electrode resolves the Schottky contact issue, and it also offers additional advantages as PMMA fills the gaps between the NFs and forms a capping layer at the top of the device. When a force is applied vertically, stress is transmitted through the capping layer to all NFs under the force application area, and this greatly improves the piezoelectric efficiency of the NGs. Furthermore, the PMMA protects the NFs from an interaction with the electrode and thereby improves the robustness of the NGs.[11]

PMMA (PMMA495-A8, Microchem) with a thickness of about 2 μm was added via dip coating between the ZnO NFs and the top ITO electrode. A typical NG with effective dimensions of 1×1 cm^2 produced an open-circuit voltage of 82 V (Fig. S4b in ESI†) and a short-circuit current density of 43 μA cm^{-2} (Fig. S4c in ESI†). The function of the PMMA and the PDMS layers in these NG devices is essentially identical, yet the output voltage and current for the devices with the PMMA coating layer was slightly lower than that for PDMS (Fig. 2c and d). This may be ascribed to a greater robustness of PDMS relative to that of PMMA. Therefore, the load will be more efficiently transferred to the NFs when a PDMS coating layer is employed.
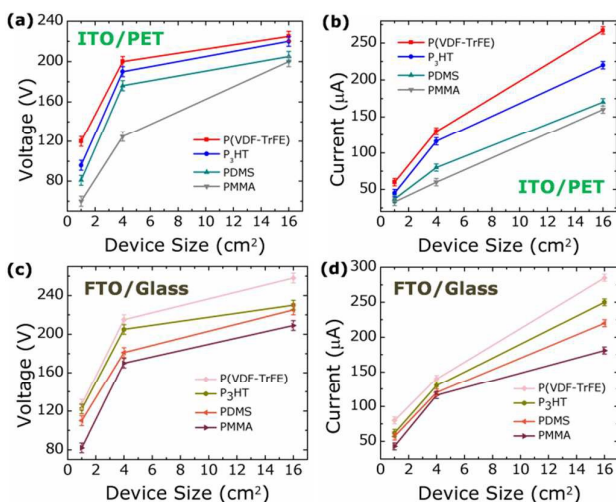
Fig. 6 Size dependency of NGs based on ZnO NFs. (a) Open-circuit voltage, and (b) short-circuit current of NG based on ZnO NFs on ITO/PET; (c, d) ZnO NFs on FTO/glass substrates with different coating materials: PMMA, PDMS, P₃HT, and P(VDF-TrFE).

p-type polymer layer

Free carriers exist in undoped ZnO due to structural defects, and these usually screen some of the piezoelectric potential that is established when ZnO is subjected to mechanical deformation. Therefore, although the output current from ZnO is much larger than that from insulating piezoelectric materials (such as PZT, PVDF, and BTO), the output voltage from ZnO is low due to the piezoelectric potential screening effect, resulting in a lower overall output power generation.[17,18] Lee *et al*. introduced a p-type polymer layer (P₃HT) between the piezoelectric semiconducting thin film and an electrode in order to minimize this effect. At the ZnO-P₃HT interface, holes from P₃HT near the interface diffuse into the ZnO layer while free electrons from ZnO diffuse into P₃HT, forming a charge-depletion interface at the p-n junction. This phenomenon greatly reduces the piezoelectric potential screening effect, and furthermore, additional carriers from conducting polymer and a shift in the Fermi level will serve to increase the power output.[17]

In our NG device, P₃HT was used as the p-type polymer. 30 mg of P₃HT was dissolved in 3 mL of chloroform and coated on piezoelectric semiconducting ZnO NFs via dip coating. A typical NG with effective dimensions of 1×1 cm^2 presented an open-circuit voltage of 122 V (Fig. S4e in ESI†) and a short-circuit current density of 62 μA cm^{-2} (Fig. S4f in ESI†). This enhancement is attributed to a reduction in the piezoelectric potential screening effect at the p-n junction of the P₃HT layer and ZnO NFs.

Hybridization of two piezoelectric materials

To ensure maximum output power, a 10-μm-thick ferroelectric P(VDF-TrFE) layer was prepared by dissolving P(VDF-TrFE) in a solvent of N,N-dimethylformamide (DMF). This was uniformly spin-coated on ZnO NFs by first coating at 0.4 wt% and then at 10 wt% (Fig. S5 in ESI†). A 127 V maximum peak open-circuit voltage (Fig. S4h in ESI†) and a short-circuit current density of 80 μA cm^{-2} (Fig. S4k in ESI†) were obtained in our 1×1 cm^2 NG. To date, these values are 3.4 times higher than the best reported output voltage (37 V); 6.6 times higher than the output current density (12 μA cm^{-2}) from integrated ZnO NW-based NGs;[11] and 3.4 times higher than the current density (23.5 μA cm^{-2}) of an ultralong PZT NW array-based NG.[25] The effective output power density (P) was calculated of ~ 1.6 mW cm^{-2}. This dramatic improvement in the output voltage and the current density may be ascribed to the hybridization of two piezoelectric materials. Lee *et al*. suggested that coupling ZnO NWs with another piezoelectric P(VDF-TrFE) component may improve the combined piezoelectric coefficient of the hybrid structure. P(VDF-TrFE) is known to have a negative piezoelectric coefficient (d_{33}) while ZnO NWs have a positive value. This difference allows a vertical alignment in the dipoles, leading to a positive output for our hybrid device and the poling process becoming unnecessary.[19] Furthermore, the thin insulating layer coated on the ZnO NFs can be fully utilized by the aforementioned methodology since the coupling effects of the hybrid piezoelectric structure will further improve the piezoelectric coefficient.

We also attempted to fabricate a flexible ZnO NF-based NG on a wearable Au-coated woven-fiber polyester textile substrate to determine the viability of such a device. A thin, self-adhesive 40-

mm-thick polyethylene (PE) film was placed on the top of the ZnO NFs, and another Au-coated textile substrate was placed on the charged PE layer as the top electrode.[10] The NGs that were fabricated in the 10 cm^2 device were tested using a sound wave as the vibration source, and Fig. 3a depicts the device structure schematic. The output power from the sound-driven textile NG was significantly enhanced as a result of the synergistic electrostatic (or triboelectric) and piezoelectric effects. Upon applying a sinusoidal sound input of 100 dB at 100 Hz, the highest open-circuit peak voltage (45 V, Fig. 3b) and the open-circuit current (15 μA, Fig. 3c) of the NGs were recorded. These values are significantly higher than the best values reported elsewhere (5.6 times higher in output voltage and 6 times higher in output current of ZnO NW-based NGs on textile substrates).[10] Instead of using an insulating PE layer, P(VDF-TrFE)-coated ZnO NFs were then employed to induce a synergistic combination of the hybridized piezoelectric materials and the insulating layer. However, the open-circuit peak voltage was significantly reduced to 4.2 V (Fig. S6a in ESI†), and the high robustness of the P(VDF-TrFE) decreased the sound-generated load that was transferred to the ZnO NFs, thus reducing the output voltage. Therefore, we believe that this response is mainly a result of the triboelectric effect between the P(VDF-TrFE)- and Au-coated textiles. In addition, an NG-based Schottky contact formed when the PE layer was removed, and 7 V open-circuit peak voltage was observed (Fig. S6b in ESI†). This output voltage is quite small compared to the output voltage of the NG (45 V) with PE(insulating layer)/ZnO NFNGs. Moreover, the screening effects on the piezoelectric potential produced via a carrier tunneling through a Schottky barrier with highly conductive ZnO NFs (as mentioned above), may also contribute to this low output voltage.

The ZnO NWs were also grown on an FTO/glass substrate by using a hydrothermal method to compare them against ZnO NF based NGs, and the recipe that was used to synthesize the ZnO NWs was reported elsewhere.[11] The ZnO NW-based NGs were also fabricated with different coating materials, and Fig. 4a shows the SEM image of pristine ZnO NWs on an FTO/glass substrate in which ZnO NWs have an average diameter of 50 nm and a length of 1 μm. The highest peak open-circuit voltage of 35 V (Fig. 4c) and a short-circuit current density of 21 μA cm^{-2} (Fig. 4d) of the NWNGs was observed in P(VDF-TrFE)-coated ZnO NWs (Fig. 4b). Although a smaller output was observed relative to that of ZnO NFs, the NWNGs exhibited tendencies that were consistent with the effect of different coating materials, as shown in Fig. 5a and b. The peak open-circuit voltage of 24 V and the short-circuit current density of 11 μA cm^{-2} for PMMA-coated ZnO NWs was slightly smaller than the reported output value (37 V) and the output current density (12 μA cm^{-2}) of the integrated NWNGs reported elsewhere.[11] This finding may be obvious: unlike the methodologies presented in those reports, free charge carriers were not separated between the NWs that we tested. Therefore, free charge carriers within the NWs partially screened the piezoelectric potential, reducing the magnitude and thereby degrading the performance of the NG.[11]

Several triboelectric NGs with PMMA, PDMS, P$_3$HT, or P(VDF-TrFE) coating layers were fabricated on FTO/glass substrates to identify the main factor that enhanced our devices. The device structures are shown in the ESI Fig. S7a.† A peak open-circuit voltage of 9 V (Fig. S7b in ESI†) and a short-circuit current density of

4 μA cm^{-2} (Fig. S7c in ESI†) were observed for the NG with a P(VDF-TrFE) coating. A slight difference in the output current and voltage of the NG-based triboelectric behavior became noticeable depending on the coating material used, as shown in Fig. 5a and b. This may be attributed to the different chemical potential of the coating materials. Thus, we believe that the triboelectric effect is mainly responsible for our findings. Even for the case where P(VDF-TrFE) coating was used, we argue that our claim is still valid due to the lack of the poling process to render a proper piezoelectricity in P(VDF-TrFE).[19]
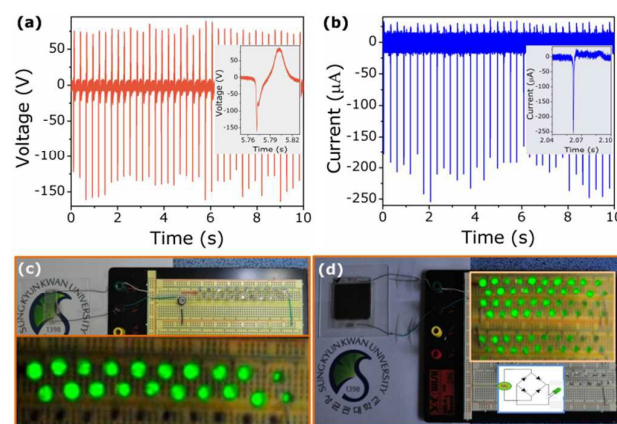
Fig. 7 (a) Open-circuit voltage, and (b) short-circuit current for a device area of 4 × 4 cm^2. Instantaneous activation of (c) 20 LEDs and (d) 60 LEDs under periodic hand compression for device areas of 1 × 1 cm^2 and 4 × 4 cm^2, respectively.

We also investigated the changes in voltage and current output for different device sizes. The NFNGs were fabricated with different device sizes: 1 × 1, 2 × 2, and 4 × 4 cm^2, and Fig. 6c and d respectively show the peak open-circuit voltage and short-circuit current of the NFs on the FTO/glass-substrate-based NGs. The peak open-circuit voltage and the short-circuit current of NFs on ITO/PET-substrate-based NGs are shown in Fig. 6a and b, respectively. The generated voltage and the current output would increase with increasing the device size because more nanoflakes available under pressing load will be exploited to generate a larger piezoelectric response in the ZnO NFNGs. However, the voltage and the current output did not increase linearly with the device size, and this may be because the applied force was held constant and reduced the force applied on a single NF as the size of the device increased. A similar tendency was also observed for NGs based on ZnO NFs on ITO/PET substrates (Fig. S8a in ESI†) with different coating materials, as shown in Fig. 6a and b. However, the overall voltage and current output of the ZnO NFs on ITO/PET substrates was lower than that of the ZnO NFs on the FTO/glass NGs, and this may result from a higher stiffness in the glass substrates compared to the PET substrates. Therefore, the piezoelectric strength of the NFs on glass was stronger, and the response was faster.

To demonstrate the viability of the NFNGs, we attempted to power a large number of LEDs. A commercial bridge rectifier was connected to the NG to convert AC to DC output, and the device was then connected to arrays of commercially available green-

Nanoscale Accepted Manuscript

emission LEDs (LSG/R/Y50343) connected in series, each with a forward voltage of 2.7 V. NFNGs with a thin insulating PDMS layer were fabricated in a device with an area of 1×1 cm^2, as shown in Fig. 7c. Under periodic compression induced by a human hand, the electric pulses and the open-circuit peak voltage generated from the NG instantaneously and simultaneously turned on all 20 LEDs (as shown in ESI Movie 1)†. A larger device of 4×4 cm^2 in size was also prepared to facilitate more efficient hand compressions, and we demonstrated that our NFNGs with a thin insulating P(VDF-TrFE) layer had a maximum peak open-circuit voltage of 258 V (Fig. 7a) and a short-circuit current with 285 µA pulses (Fig. 7b). Under periodic hand compression, this device could instantaneously and simultaneously activate more than 60 LEDs, as shown in Fig. 7d (and in ESI Movie 2)†. Therefore, this successful demonstration of the use of NFNGs indicates that our novel structure has great potential for applications of ZnO NFs targeting self-powered systems.

Conclusions

We have developed a novel ZnO NF structure for NGs with an ultrahigh output power. The performance of these NG devices was systematically investigated with respect to different vibration sources, interface mechanisms, ZnO morphologies, and device sizes. The output from the NFNGs reached up to 127 V for the output open-circuit voltage and 80 µA cm^{-2} for the short-circuit current density, with a maximum output power density of 1.6 mW cm^{-2}. This is the highest output power value achieved to date with ZnO-based piezoelectric NGs. We believe that the enhanced performance can be attributed to the high surface area and the strong surface piezoelectricity of the ZnO NF structure. Our results suggest that these NFNGs have structures that are highly promising for use in future flexible, transparent self-powered NGs targeting sensor device applications.

Acknowledgements

References

1   Z. L. Wang, *Adv. Mater.,* 2012, **24**, 4632–4646.
2   G. Zhu, Z. H. Lin, Q. Jing, P. Bai, C. Pan, Y. Yang, Y. Zhou, and Z. L. Wang, *Nano Lett.,* 2013, **13**, 847–853.
3   X. S. Zhang, M. D. Han, R. X. Wang, F. Y. Zhu, Z. H. Li, W. Wang and H. X. Zhang, *Nano Lett.,* 2013, **13**, 1168–1172.
4   S. Wang, L. Lin and Z. L. Wang, *Nano Lett.,* 2012, **12**, 6339–6346.
5   Y. Xi, J. Song, S. Xu, R. Yang, Z. Gao, C. Hu and Z. L. Wang, *J. Mater. Chem.,* 2009, **19**, 9260–9264.
6   Z. L. Wang and J. Song, *Science,* 2006, **312**, 242–246.
7   X. Wang, J. Song, J. Liu and L. W. Zhong, *Science,* 2007, **316**, 102–105.
8   Y. Gao and Z. L. Wang, *Nano Lett.,* 2007, **7**, 2499–2505.
9   R. Yang, Y. Qin, L. Dai and Z. L. Wang, *Nat. Nanotechnol.,* 2009, **4**, 34–39.

10 H. Kim, S. M. Kim, H. Son, B. Park, J. Ku, J. I. Sohn, K. Im, J. E. Jang, J. J. Park, O. Kim, S. Cha and Y. J. Park, *Energ. Environ. Sci.,* 2012, **5**, 8932–8936.
11 G. Zhu, A. C. Wang, Y. Liu, Y. Zhou and Z. L. Wang, *Nano Lett.,* 2012, **12**, 3086–3090.
12 Y. Hu, Y. Zhang, C. Xu, G. Zhu and Z. L. Wang, *Nano Lett.,* 2010, **10**, 5025–5031.
13 G. Zhu, R. Yang, S. Wang and Z. L. Wang, *Nano Lett.,* 2010, **10**, 3151–3155.
14 Y. Hu, Y. Zhang, C. Xu, L. Lin, R. L. Snyder and Z. L. Wang, *Nano Lett.,* 2011, **11**, 2572–2577.
15 Y. Hu, C. Xu, Y. Zhang, L. Lin, R. L. Snyder and Z. L. Wang, *Adv. Mater.,* 2011, **23**, 4068–4071.
16 S. Lu, Q. Liao, J. Qi, S. Liu, Y. Liu, Q. Liang, G. Zhang, Y. Zhang, *Nano Res.*, 2015, 1-8.
17 K. Y. Lee, B. Kumar, J. S. Seo, K. H. Kim, J. I. Sohn, S. N. Cha, D. Choi, Z. L. Wang and S. W. Kim, *Nano Lett.,* 2012, **12**, 1959–1964.
18 B. Kumar and S. W. Kim, *Nano Energy,* 2012, **1**, 342–355.
19 M. Lee, C. Y. Chen, S. Wang, S. N. Cha, Y. J. Park, J. M. Kim, L. J. Chou and Z. L. Wang, *Adv. Mater.,* 2012, **24**, 1759–1764.
20 Z. Zhang, Q. Liao, X. Yan, Z. L. Wang, W. Wang, X. Sun, P. Lin, Y. Huang and Y. Zhang, *Nano Res.*, 2014, **7**, 190-198.
21 Q. Liao, Z. Zhang, X. Zhang, M. Mohr, Y. Zhang and H.-J. Fecht, *Nano Res.*, 2014, **7**, 917-928.
22 C. Falconi, G. Mantini, A. D'Amico and Z. L. Wang, *Sensor. Actuat. B-Chem.,* 2009, **139**, 511–519.
23 Z. Yan and L. Y. Jiang, *Europhys. Lett.,* 2012, **99**, 27007.
24 J. Zhang and C. Wang, *J. Appl. Phys.,* 2012, **111**, 094303.
25 L. Gu, N. Cui, L. Cheng, Q. Xu, S. Bai, M. Yuan, W. Wu, J. Liu, Y. Zhao, F. Ma, Y. Qin and Z. L. Wang, *Nano Lett.,* 2013, **13**, 91–94.
26 P. K. Yang, L. Lin, F. Yi, X. Li, K. C. Pradel, Y. Zi, C. I. Wu, J. H. He, Y. Zhang and Z. L. Wang, *Adv. Mater.,* 2015, **27**, 3817-3824.
27 C. Q. Chen, Y. Shi, Y. S. Zhang, J. Zhu and Y. Yan, *J. Phys. Rev. Lett.* 2006, **96**, 075505.
28 G. Stan, C. V. Ciobanu, P. M. Parthangal and R. F. Cook, *Nano Lett.,* 2007, **7**, 3691–3697.
29 A. J. Kulkarni, M. Zhou and F. J. Ke, *Nanotechnology,* 2005, **16**, 2749–2756.
30 M. H. Zhao, Z. L. Wang and S. X. Mao, *Nano Lett.,* 2004, **4**, 587–590.
31 A. K. Tagantsev, *Phys. Rev. B,* 1986, **34**, 5883–5889.
32 K.-H. Kim, B. Kumar, K. Y. Lee, H.-K. Park, J.-H. Lee, H. H. Lee, H. Jun, D. Lee and S.-W. Kim, *Sci. Rep.,* 2013, **3**, 2017.
33 J. I. Sohn, S. N. Cha, B. G. Song, S. Lee, S. M. Kim, J. Ku, H. J. Kim, Y. J. Park, B. L. Choi, Z. L. Wang, J. M. Kim and K. Kim, *Energ. Environ. Sci.,* 2013, **6**, 97–104.
34 M. K. Gupta, J.-H. Lee, K. Y. Lee and S.-W. Kim, *ACS Nano,* 2013, **7**, 8932–8939.
35 B. Kumar and S. W. Kim, *J. Mater. Chem.,* 2011, **21**, 18946–18958.